J|A|C|S
ARTICLES
Published on Web 05/23/2002

Mechanism of C−H Bond Activation/C−C Bond Formation Reaction between Diazo Compound and Alkane Catalyzed by Dirhodium Tetracarboxylate

Eiichi Nakamura,* Naohiko Yoshikai, and Masahiro Yamanaka†

Contribution from the Department of Chemistry, The University of Tokyo, Bunkyo-ku, Tokyo 113-0033, Japan

Received December 19, 2001

Abstract: The B3LYP density functional studies on the dirhodium tetracarboxylate-catalyzed C−H bond activation/C−C bond formation reaction of a diazo compound with an alkane revealed the energetics and the geometry of important intermediates and transition states in the catalytic cycle. The reaction is initiated by complexation between the rhodium catalyst and the diazo compound. Driven by the back-donation from the Rh $4d_{xz}$ orbital to the C−N σ^*-orbital, nitrogen extrusion takes place to afford a rhodium−carbene complex. The carbene carbon of the complex is strongly electrophilic because of its vacant 2p orbital. The C−H activation/C−C formation proceeds in a single step through a three-centered hydride transfer-like transition state with a small activation energy. Only one of the two rhodium atoms works as a carbene binding site throughout the reaction, and the other rhodium atom assists the C−H insertion reaction. The second Rh atom acts as a mobile ligand for the first one to enhance the electrophilicity of the carbene moiety and to facilitate the cleavage of the rhodium−carbon bond. The calculations reproduce experimental data including the activation enthalpy of the nitrogen extrusion, the kinetic isotope effect of the C−H insertion, and the reactivity order of the C−H bond.

Carbon−carbon bond forming reactions that rely on catalytic activation of the C−H bond in a saturated hydrocarbon have become standard synthetic protocols.[1,2] Among them, the reaction of an α-diazoester catalyzed by a dirhodium tetracarboxylate or a related catalyst is the reaction widely utilized as a practical synthetic method (Scheme 1).[3] In an ideal case, a new C−C bond between two sp^3 carbon centers is created through activation of the C−H bond of a saturated hydrocarbon in a diastereo- and enantioselective manner.[4]

It has been generally assumed that the reaction involves a rhodium−carbene complex and that the catalytic cycle consists of three steps, Rh-catalyzed nitrogen extrusion from the diazo compound, C−H activation, and C−C bond formation. The latter two steps are assumed to take place more or less as a single reaction (Scheme 1).[3] The first step is rate limiting for secondary C−H insertion,[5] and hence the mechanistic information on the subsequent steps is scarce, generating various speculations. In addition, there has been scarcity of discussions

Scheme 1. Schematic Representation of the Catalytic Cycle of the Rhodium Tetracarboxylate-Catalyzed C−H Bond Activation/C−C Bond Forming Reaction of an α-Diazoacetate with an Alkane

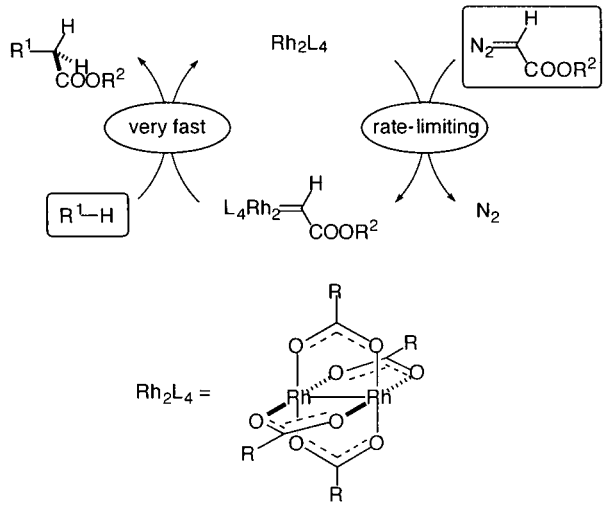

* To whom correspondence should be addressed. E-mail: nakamura@chem.s.u-tokyo.ac.jp.
† Present address: Department of Applied Chemistry, Tokyo Institute of Technology, Meguro-ku, Tokyo 152-8550, Japan.

(1) (a) Shilov, A. E.; Shul'pin, G. B. *Chem. Rev.* **1997**, *97*, 2879−2932. (b) Dyker, G. *Angew. Chem., Int. Ed.* **1999**, *38*, 1698−1712.
(2) (a) *Selective Hydrocarbon Activation*; Davies, J. A., Watson, P. L., Greenberg, A., Liebman, J. F., Eds.; VCH Publishers: New York, 1990. (b) *Activation and Functionalization of Alkanes*; Hill, C. L., Ed.; John Wiley & Sons: New York, 1989. (c) Kakiuchi, F.; Murai, S. In *Activation of Unreactive Bonds and Organic Synthesis*; Murai, S., Ed.; Splinger: Berlin, 1999.
(3) (a) Doyle, M. P. *Chem. Rev.* **1986**, *86*, 919−939. (b) Taber, D. F. In *Comprehensive Organic Synthesis*; Trost, B. M., Fleming, I., Eds.; Pergamon Press: New York, 1991; Vol. 3, Chapter 4.2. (c) Doyle, M. P. In *Comprehensive Organometallic Chemistry II*; Hegedus, L. S., Ed.; Pergamon Press: New York, 1995; Vol. 12, Chapters 5.1 and 5.2. (d) Ye, T.; McKervey, M. A. *Chem. Rev.* **1994**, *94*, 1091−1160. (e) Doyle, M. P.; McKervey, M. A.; Ye, T. *Modern Catalytic Methods for Organic Synthesis with Diazo Compounds*; John Wiley & Sons: New York, 1998. (f) Dörwald, F. Z. *Metal Carbenes in Organic Synthesis*; Wiley-VCH: Weinheim, 1999.
(4) (a) Davies, H. M. L.; Antoulinakis, E. G. *J. Organomet. Chem.* **2001**, *617*−*618*, 47−55. (b) Doyle, M. P.; Forbes, D. C. *Chem. Rev.* **1998**, *98*, 911−935.
(5) (a) Alonso, M. E.; García, M. del C. *Tetrahedron* **1989**, *45*, 69−76. (b) Pirrung, M. C.; Morehead, A. T., Jr. *J. Am. Chem. Soc.* **1996**, *118*, 8162−8163. Pirrung, M. C.; Liu, H.; Morehead, A. T., Jr. *J. Am. Chem. Soc.* **2002**, *124*, 1014−1023.

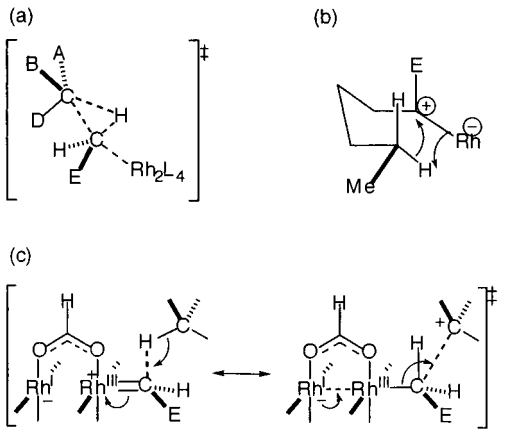

Figure 1. Transition state models of C−H bond activation with dirhodium−carbene complex described by Doyle (a), Taber (b), and this work (c).

about such fundamental issues as the roles of the dinuclear structure of the catalyst that appears to be responsible for the unique success of the dirhodium catalyst, and the function of the bridging carboxylates (except their known ability to harness chiral centers).

Although the majority of previous reports on the rhodium-catalyzed C−H activation/C−C formation reaction focused on synthetic applications, there exist several data that provide information on the reaction mechanism: (1) The activation enthalpy of the $Rh_2(OAc)_4$-catalyzed nitrogen extrusion reaction of ethyl diazoacetate ($\Delta H^{\ddagger} = 16.4 \pm 1.4$ kcal/mol) that is the rate-limiting step of the catalytic cycle for secondary C−H insertion,[5a] (2) $^1H/^2H$ kinetic isotope effects (KIEs) of the C−H bond activation,[6] which have been shown to depend on the nature of the carboxylate ligands in the rhodium catalyst, (3) qualitative structure/reactivity correlation indicating a reactivity order of primary ≪ secondary < tertiary C−H bond[7] and the enhanced reactivity of a C−H bond adjacent to a heteroatom,[8] (4) carboxylate ligand effects on the regio- and stereoselectivity of the C−H insertion reaction,[9] and (5) retention of the configuration of the carbon at which the C−H activation occurs.[10]

On the basis of the facts listed above and the stereochemical outcomes of intra- and intermolecular C−H insertion reactions, various working models of the transition state (TS) of the C−H bond activation process have been proposed.[7b,11] Representative examples are illustrated in Figure 1. Figure 1a illustrates a three-centered concerted transition state of the C−H activation, which was described by Doyle et al. and now is widely accepted.[7b] Figure 1b illustrates a four-centered hypothesis by Taber et al., where an interaction between the hydrogen atom and the rhodium atom is assumed.[11a] A three-centered mechanism involving a stepwise character was also suggested.[9b]

For further development of the C−H activation chemistry, it was felt that deeper understanding of the reaction mechanism was indispensable. We report herein the pathways of the rhodium-catalyzed reactions of diazomethane and methyl diazoacetate as revealed by density functional calculations. The reaction pathways that we propose in this article provide the first qualitative to semiquantitative account of the experimental data, as well as the structures of important intermediates and TSs involved in the catalytic cycle. With respect to the crucial C−H insertion step, we have found that two important events are involved in the transition state (Figure 1c). One is hydride transfer from the alkane to the carbene carbon, and the other is regeneration of the Rh−Rh bond and formation of a new C−C bond, as depicted as two resonance structures in Figure 1c. While the reaction is concerted, not stepwise, it is markedly nonsynchronous, with hydride transfer preceding C−C bond formation. The theoretical analyses of the properties of intermediates and TSs revealed unique roles of the rhodium catalyst that originate from its dimetallic structure.

Chemical Models

In the present studies, we employed dirhodium tetraformate (**I**) as a model of a common catalyst, dirhodium tetraacetate, in the interest of computational facility. With this model catalyst, two model catalytic reactions were studied. One was the reaction of diazomethane with methane or propane (CH_2 insertion, eq 1). This reaction has not been reported in the literature. Nonetheless, this simple model was investigated to understand the fundamental characters of the dirhodium−carbene complex and the mechanism of its C−H insertion reaction. The central mechanistic principle established with this model was found to hold also in a more realistic reaction model. The reaction of methyl diazoacetate with methane or propane (CH_3 and CH_2 insertion) was also studied (eq 2). This system is much more relevant to the actual synthetic reactions. Unlike the relatively unreactive substrates such as methane and propane, SiH_4 and dimethyl ether reacted with the rhodium carbene complex without any activation energy.[12] A 1:1 stoichiometry of the rhodium catalyst and the diazo compound was assumed on the basis of the kinetic study by Pirrung et al.[5b]

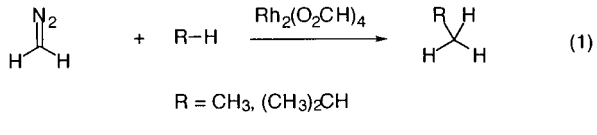

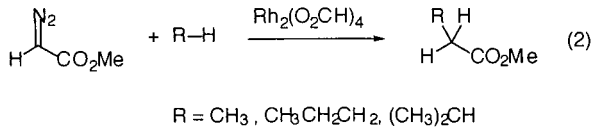

Computational Method

All calculations were performed with Gaussian 94[13] and Gaussian 98[14] packages. The density functional theory (DFT) method was employed using the B3LYP hybrid functional.[15] Structures were

(6) (a) Demondeceau, A.; Noels, A. F.; Costa, J.-L. *J. Mol. Catal.* **1990**, *58*, 21−26. (b) Wang, P.; Adams, J. *J. Am. Chem. Soc.* **1994**, *116*, 3296−3305.
(7) (a) Taber, D. F.; Ruckle, R. E., Jr. *J. Am. Chem. Soc.* **1986**, *108*, 7686−7693. (b) Doyle, M. P.; Westrum, L. J.; Wolthuis, W. N. E.; See, M. M.; Boone, W. P.; Bagheri, V.; Pearson, M. M. *J. Am. Chem. Soc.* **1993**, *115*, 958−964.
(8) Adams, J.; Spero, D. M. *Tetrahedron* **1991**, *47*, 1765−1808.
(9) (a) Padwa, A.; Austin, D. J.; Price, A. T.; Semones, M. A.; Doyle, M. P.; Protopopova, M. N.; Winchester, W. R.; Tran, A. *J. Am. Chem. Soc.* **1993**, *115*, 8669−8680. (b) Pirrung, M. C.; Morehead, A. T., Jr. *J. Am. Chem. Soc.* **1994**, *116*, 8991−9000. (c) Wang, J.; Chen, B.; Bao, J. *J. Org. Chem.* **1998**, *63*, 1853−1862.
(10) Taber, D. F.; Petty, E. H.; Raman, K. *J. Am. Chem. Soc.* **1985**, *107*, 196−199.
(11) (a) Taber, D. F.; You, K. K.; Rheingold, A. L. *J. Am. Chem. Soc.* **1996**, *118*, 547−556. (b) Taber, D. F.; Malcolm, S. C. *J. Org. Chem.* **1998**, *63*, 3717−3721.
(12) These results are consistent with the fact that a C−H bond adjacent to an oxygen atom and a Si−H bond is 10^3-10^4 times more reactive than a C−H bond of a normal hydrocarbon: Davies, H. M. L.; Hansen, T.; Churchill, M. R. *J. Am. Chem. Soc.* **2000**, *122*, 3063−3070.

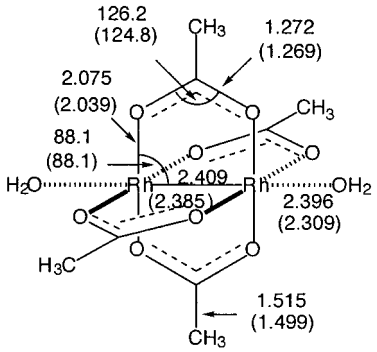

Figure 2. The structure of $Rh_2(OAc)_4 \cdot 2H_2O$. The numbers refer to bond lengths (Å) and bond angles (deg) optimized at the B3LYP/631LAN level (C_1 symmetry). The X-ray crystallographic data are shown in parentheses.

optimized with a basis set (denoted as 631LAN) consisting of the LANL2DZ basis set including a double-ζ valence basis set with the Hay and Wadt effective core potential (ECP)[16] for Rh and the 6-31G-(d) basis set[17] for C, H, N, and O. The method and the basis sets used here are known to give reliable results for transition metal reactions including rhodium (carbene) complexes.[18,19] Stability of the Kohn−Sham solution was confirmed by stability analyses[20] for representative stationary points. Some stationary points were optimized with symmetry assumption (vide infra). The structures of **I** and **V** (methylene carbene complex of **I**) optimized at the B3LYP/631LAN level show good agreement with those optimized at the MP2(FC)/631LAN level.[21] The B3LYP/631LAN level calculation of $Rh_2(OAc)_4 \cdot 2H_2O$ reproduced the X-ray crystallographic data of the same compound.[22] Figure 2 illustrates the structure and mean structural parameters of the complex. The differences between computational and experimental data for representative parameters are as follows: Rh−Rh (1.0%), Rh−O (carboxylate, 1.8%), Rh−O (H_2O, 3.7%), C−C (1.1%), C−O (0.3%).

Each stationary point was adequately characterized by normal coordinate analysis (no imaginary frequencies for an equilibrium structure and one imaginary frequency for a transition structure). The intrinsic reaction coordinate (IRC) analysis[23] was carried out throughout the reaction pathways to confirm that all stationary points are smoothly connected to each other. Enthalpies and Gibbs free energies were obtained on the basis of the calculated frequencies scaled by 0.9614.[24,25] Electronic energies will be discussed first, and enthalpies and Gibbs free energies will be discussed second. To evaluate the effect of the solvent polarity on the energetics of the diazomethane model, a single-point energy calculation was performed with self-consistent reaction field (SCRF) method (based on the polarized continuum model (PCM),[26] $\epsilon = 8.93$ for CH_2Cl_2) on the gas-phase geometry. With the scaled frequencies,[24,25] kinetic isotope effects (KIE) were computed by Bigeleisen−Mayer's equation[27] with Wigner tunnel correction. It should be pointed out that the calculations give us only the stationary points on the potential surface of electronic energy. As will be discussed in detail, the entropy changes in this reaction are too large to be neglected. Thus, the structures reported here (especially C−H insertion transition states) may not necessarily be close to those of the stationary points on the potential surface of Gibbs free energy. However, reasonable agreement of calculated and experimental data such as the value of KIE suggests that the optimized transition structures of C−H insertion reflect the reality. The Boys localization procedure[28] was performed to obtain localized Kohn−Sham orbitals[29] (LOs). Natural population analysis and natural bond orbital (NBO) analysis were performed at the same level as the one used for geometry optimization.[30] All charge distribution analyses discussed throughout this article are made on the basis of the natural population analysis.

Results

1. Reaction of Diazomethane with Methane and Propane. (a) Reaction Pathways and Energetics. We first investigated the reactions of diazomethane with methane and propane as basic model reactions. In Scheme 2 (R = H) and Figure 3 are shown the reaction course and the energy profile of the C−H insertion reaction of diazomethane with methane and propane catalyzed by $Rh_2(O_2CH)_4$ (**I**). The catalytic cycle involves seven steps: First, **I** and diazomethane interact to form a Rh/diazomethane complex **II** with a 19.9 kcal/mol stabilization energy. Nitrogen extrusion then proceeds via **TS-III** with a 16.6 kcal/mol activation energy, which is followed by the formation of a rhodium−methylene carbene complex **V**. After **TS-III**, there exists a weak complex (**IV**) between **V** and dinitrogen (2.1 kcal/mol more stable than **TS-III**). The next step toward the final product first involves a **V**/alkane complex **VIa** (methane reaction is denoted as **a**, 0.2 kcal/mol stabilization)

(13) Frisch, M. J.; Trucks, G. W.; Schlegel, H. B.; Gill, P. M. W.; Johnson, B. G.; Robb, M. A.; Cheeseman, J. R.; Keith, T.; Petersson, G. A.; Montogomery, J. A.; Raghavachari, K.; Al-Laham, M. A.; Zakrzewski, V. G.; Ortiz, J. V.; Foresman, J. B.; Cioslowski, J.; Stefanov, B. B.; Nanayakkara, A.; Challacombe, M.; Peng, C. Y.; Ayala, P. Y.; Chen, W.; Wong, M. W.; Andres, J. L.; Replogle, E. S.; Gomperts, R.; Martin, R. L.; Fox, D. J.; Binkley, J. S.; Defrees, D. J.; Baker, J.; Stewart, J. P.; Head-Gordon, M.; Gonzalez, C.; Pople, J. A. *Gaussian 94*, revision D.3; Gaussian, Inc.: Pittsburgh, PA, 1995.
(14) Frisch, M. J.; Trucks, G. W.; Schlegel, H. B.; Scuseria, G. E.; Robb, M. A.; Cheeseman, J. R.; Zakrzewski, V. G.; Montogomery, J. A., Jr.; Stratmann, R. E.; Burant, J. C.; Dapprich, S.; Millam, J. M.; Daniels, A. D.; Kudin, K. N.; Strain, M. C.; Farkas, O.; Tomasi, J.; Barone, V.; Cossi, M.; Cammi, R.; Mennucci, B.; Pomelli, C.; Adamo, C.; Clifford, S.; Ochterski, J.; Petersson, G. A.; Ayala, P. Y.; Cui, Q.; Morokuma, K.; Malick, D. K.; Rabuck, A. D.; Raghavachari, K.; Foresman, J. B.; Cioslowski, J.; Ortiz, J. V.; Stefanov, B. B.; Liu, G.; Liashenko, A.; Piskorz, P.; Komaromi, I.; Gomperts, R.; Martin, R. L.; Fox, D. J.; Keith, T.; Al-Laham, M. A.; Peng, C. Y.; Nanayakkara, A.; Gonzalez, C.; Challacombe, M.; Gill, P. M. W.; Johnson, B. G.; Chen, W.; Wong, M. W.; Andres, J. L.; Head-Gordon, M.; Replogle, E. S.; Pople, J. A. *Gaussian 98*, revision A.9; Gaussian, Inc.: Pittsburgh, PA, 1998.
(15) (a) Becke, A. D. *J. Chem. Phys.* **1993**, *98*, 5648−5652. (b) Lee, C.; Yang, W.; Parr, R. G. *Phys. Rev. B* **1988**, *37*, 785−789.
(16) Wadt, W. R.; Hay, P. J. *J. Chem. Phys.* **1985**, *82*, 299−310.
(17) Hehre, W. J.; Radom, L.; Schleyer, P. v R.; Pople, J. A. *Ab Initio Molecular Orbital Theory*; John Wiley & Sons: New York, 1986 and references cited therein.
(18) Niu, S.; Hall, M. B. *Chem. Rev.* **2000**, *100*, 353−405.
(19) (a) Padwa, A.; Snyder, J. P.; Curtis, E. A.; Sheehan, S. M.; Worsencroft, K. J.; Kappe, C. O. *J. Am. Chem. Soc.* **2000**, *122*, 8155−8167. Sheehan, S. M.; Padwa, A.; Snyder, J. P. *Tetrahedron Lett.* **1998**, *39*, 949−952. (b) Schmid, R.; Herrmann, W. A.; Frenking, G. *Organometallics* **1997**, *16*, 701−708.
(20) (a) Seeger, R.; Pople, J. A. *J. Chem. Phys.* **1977**, *66*, 3045−3050. (b) Bauernschmitt, R.; Ahlrichs, R. *J. Chem. Phys.* **1996**, *104*, 9047−9052.
(21) MP2(FC) (FC = frozen core): Møller, C.; Plesset, M. S. *Phys. Rev.* **1934**, *46*, 618−622. Pople, J. A.; Krishman, R.; Schlegel, H. B.; Binkley, J. S. *Int. J. Quantum Chem. Symp.* **1979**, *13*, 225−241.
(22) Cotton, F. A.; Deboer, B. G.; Laprade, M. D.; Pipal, J. R.; Ucko, D. A. *Acta Crystallogr.* **1971**, *B27*, 1664−1671.
(23) (a) Fukui, K. *Acc. Chem. Res.* **1981**, *14*, 363−368. (b) Gonzalez, C.; Schlegel, H. B. *J. Chem. Phys.* **1989**, *90*, 2154−2161. Gonzalez, C.; Schlegel, H. B. *J. Phys. Chem.* **1990**, *94*, 5523−5527.
(24) Scott, A. P.; Radom, L. *J. Phys. Chem.* **1996**, *100*, 16502−16513.
(25) A referee suggested that the scaling factor determined for the 6-31G(d) basis set may be inappropriate for the composite basis set employed here (631LAN). However, we used the scaling factor because the frequencies of the vibration including C, H, and O atoms must have the largest effect on the KIE value of the C−H activation stage.
(26) Miertus, S.; Scrocco, E.; Tomasi, J. *J. Chem. Phys.* **1981**, *55*, 117−129. Miertus, E.; Tomasi, J. *J. Chem. Phys.* **1982**, *65*, 239−245. Barone, V.; Cossi, M.; Tomasi, J. *J. Comput. Chem.* **1998**, *19*, 404−417.
(27) Bigeleisen, J.; Mayer, M. G. *J. Chem. Phys.* **1947**, *15*, 261−267. Bigeleisen, J.; Wolfsberg, M. *Adv. Chem. Phys.* **1958**, *1*, 15−76. See also: Yamataka, H.; Nagase, S. *J. Am. Chem. Soc.* **1998**, *120*, 7530−7536.
(28) (a) Boys, S. F. In *Quantum Theory of Atoms, Molecules, and the Solid State*; Lowdin, P. O., Ed.; Academic Press: New York, 1968; pp 253−262. (b) Haddon, R. C.; Williams, G. R. J. *Chem. Phys. Lett.* **1976**, *42*, 453−455.
(29) Kohn, W.; Sham, L. J. *Phys. Rev.* **1965**, *140*, A1133−1138.
(30) Reed, A. E.; Weinstock, R. B.; Weinhold, F. *J. Chem. Phys.* **1985**, *83*, 735−746. Reed, A. E.; Curtiss, L. A.; Weinhold, F. *Chem. Rev.* **1988**, *88*, 899−926. NBO Version 3.1 in the Gaussian 98 package implemented by Glendening, E. D.; Reed, A. E.; Carpenter, J. E.; Weinhold, F. University of Wisconsin: Madison, WI, 1990.

Scheme 2. Pathway of the $Rh_2(O_2CH)_4$-Catalyzed C−H Bond Activation/C−C Bond Formation Reaction of a Diazo Compound and an Alkane

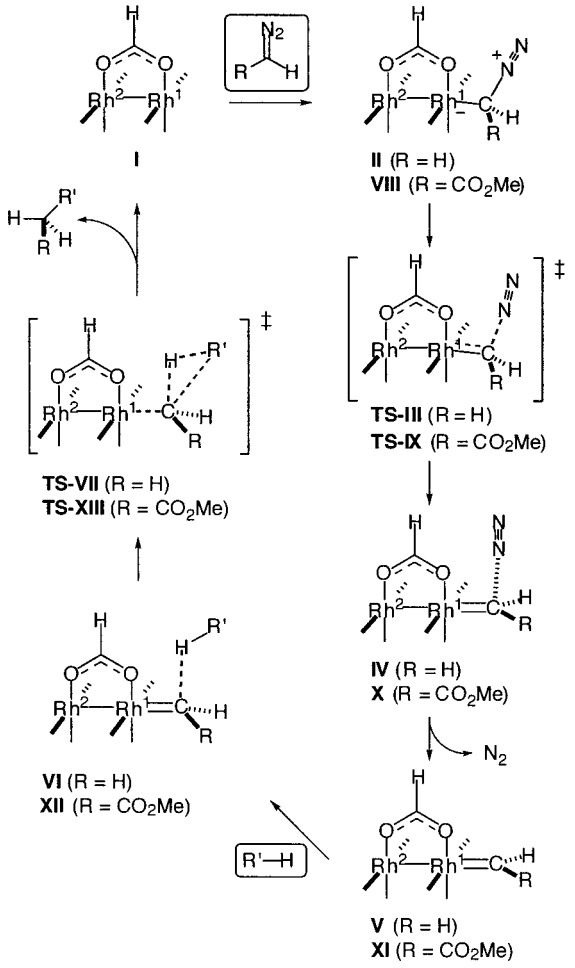

or **VIb** (propane reaction (CH_2 insertion) is denoted as **b**, 2.3 kcal/mol stabilization). C−H activation/C−C formation then takes place through **TS-VIIa** or **TS-VIIb** with a small activation energy (5.9 kcal/mol for **TS-VIIa** and 0.2 kcal/mol for **TS-VIIb**) followed by a downhill path to the final product with large exothermicity (60−62 kcal/mol), and the catalyst is regenerated. In **TS-VII**, the C−H bond activation and the C−C bond formation take place in a single step. No intermediates were located near **TS-VII** along the intrinsic reaction coordinate.

To probe the solvent effect on the reaction energetics, SCRF calculations (PCM) were performed on the gas-phase geometry (Figure 3, in parentheses). Dichloromethane ($\epsilon = 8.93$) was investigated because it is frequently used for the C−H insertion reaction.[3] The energy profile did not change very much from the one in the gas-phase calculations. Thus, the reaction is expected not to be affected by the solvent polarity as much as by coordination of basic solvent molecules to the rhodium atoms.[5b]

The 3-D structures of representative stationary points are shown in Figure 4.[31] The Rh^1-Rh^2 bond of **I** gradually becomes elongated toward the formation of the carbene complex **V** (2.400 → 2.482 Å, 3.4% increase). The Rh^1-C^1 bond of **II** (2.247 Å) significantly shortens in the nitrogen extrusion stage **TS-III**

(31) Symmetries of stationary points are as follows: **I**, D_{4h}; **V**, C_{2v}; **II**, **TS-III**, **VI**, **TS-VII**, C_s.

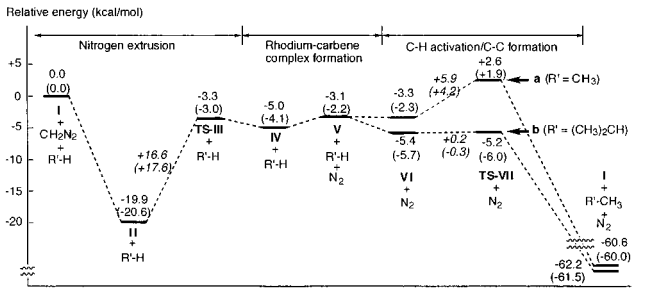

Figure 3. Energy profile of the $Rh_2(O_2CH)_4$-catalyzed reaction of diazomethane with methane (denoted as **a**) and propane (CH_2 insertion, denoted as **b**) at the B3LYP/631LAN level. The result of single-point energy calculations with the SCRF method based on the polarized continuum model ($\epsilon = 8.93$ for CH_2Cl_2) is shown in parentheses.

(1.981 Å, 11.8% decrease), which indicates that **TS-III** has the character of the carbene complex **V** (Rh^1-C, 1.906 Å).

Analysis of the charge distribution during the reaction course was found to be informative, and showed strong parallelism between this simple model (Figure 5a) and the more realistic diazoacetate model discussed later (Figure 5b). The dinitrogen moiety releases negative charge (+0.03 → +0.23) upon formation of **II**, and the negative charge moves largely into the Rh^2 atom (+0.92 → +0.81) and the carboxylate groups (−1.84 → −1.91). In the nitrogen extrusion stage (**TS-III**), the nitrogen moiety becomes less positive (+0.23 → +0.13), and the methylene group becomes cationic (0.00 → +0.09). The carboxylate groups become less negatively charged (−1.91 → −1.84), while the negative charge accumulates on the Rh^2 atom (+0.81 → +0.72). These are consistent with Pirrung's results[5b] that (1) a diazo compound strongly binds to the rhodium catalyst as the electrophilicity of carboxylate ligands increases, and (2) the nitrogen extrusion step is decelerated by highly electrophilic carboxylate ligands.

In the carbene complex **V**, the methylene moiety is positively charged (+0.19), because the negative charge moves largely from the σ-type orbital of the methylene carbon into the Rh^2 atom (increased electron occupancy of the $4d_{z^2}$ orbital during conversion from **II** to **V**). The charge of the Rh^1 atom changes little during the carbene complex formation (+0.87 ∼ +0.92). The carboxylate groups of **V** are less negatively charged (−1.79) as compared to those of catalyst **I** (−1.84), which is considered to be induced by the back-donation from the Rh^1 atom to the methylene group.

In the reaction of **V** with methane, a weak complex **VIa** is formed first with little stabilization energy (0.2 kcal/mol). In **VIa**, the distance between the carbene carbon and the methane hydrogen is very long (2.462 Å), and methane has little influences on the geometry and the charge distribution of the original carbene complex **V**.

In the C−H insertion TS (**TS-VIIa**), the Rh^1-Rh^2 bond shortens (2.482 Å → 2.460 Å), and the Rh^2 atom loses negative charge (+0.68 → +0.74). The methane moiety becomes positively charged (increase by +0.40) because of loss of the C−H σ-bonding electrons (hydride transfer to the carbene carbon). Some negative charge is also transferred to the four formate groups (−0.12 all together). In this TS, the hydride transfer from methane is half complete (the forming C^1-H bond being 1.244 Å, the carbene carbon being partially pyramidalized). The C−C bond formation (C^1-C^2 distance, 2.134 Å) lags behind the hydride transfer, and hence one can conclude that

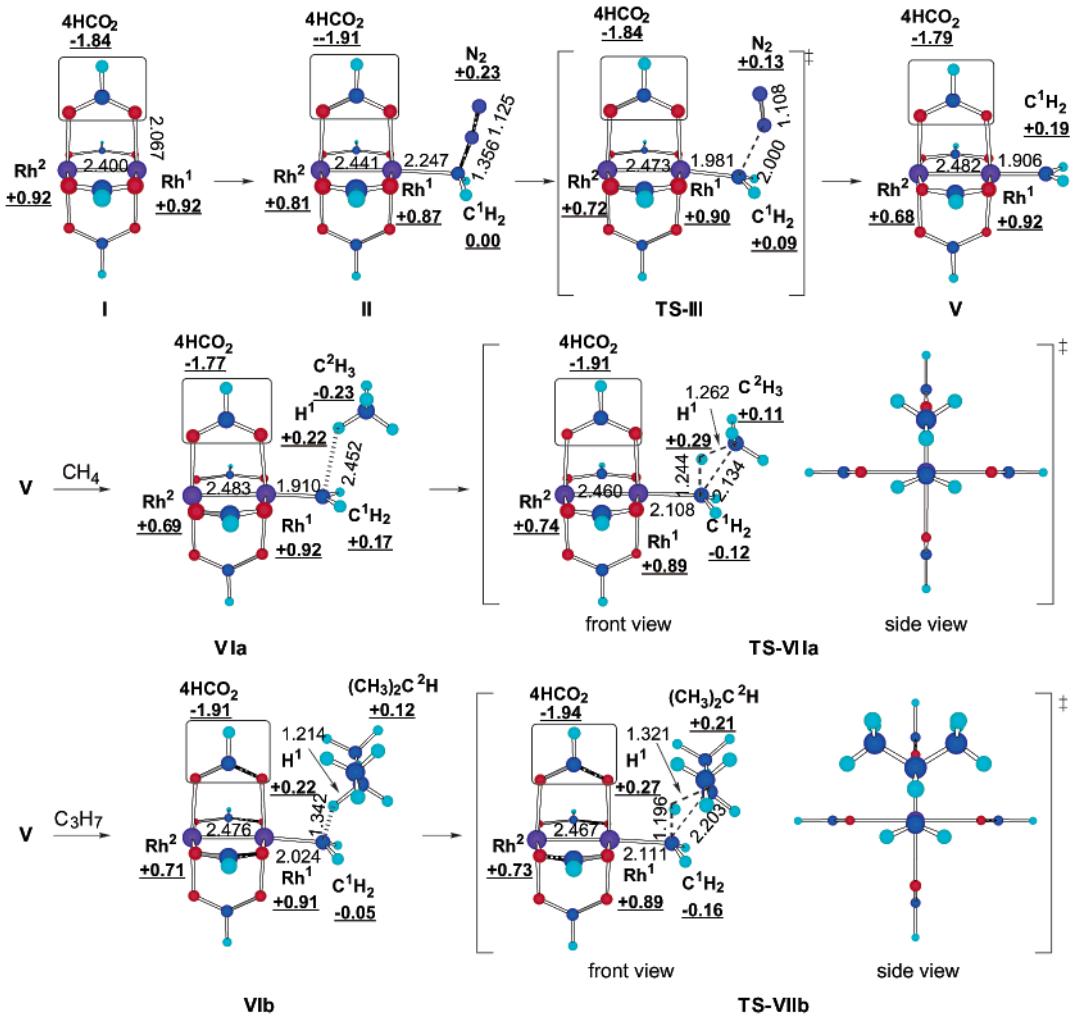

Figure 4. B3LYP/631LAN structures of stationary points in the C−H insertion reaction of diazomethane with methane and propane (at the CH_2 part). The numbers refer to bond length (Å) and natural charges (underlined).

the C−H bond activation/C−C bond formation process is a nonsynchronous concerted reaction. It should be noted that the Rh^1-C^1 bond is significantly elongated in the C−H insertion stage (1.906 Å (**V**) → 2.108 Å (**TS-VIIa**), 10.6% increase).

In the CH_2 insertion reaction with propane, the carbene complex part of **VIb** looks much different from that of **V**. The Rh^1-C^1 bond is elongated (1.906 Å → 2.024 Å), and the carbene carbon is being pyramidalized (sum of the bond angles around C^1, 350.0°). A considerable negative charge is transferred from propane to the methylene moiety (the charge of the methylene moiety, +0.19 (**V**) → −0.05 (**VIb**)). **TS-VIIb** is again a three-centered hydride transfer TS, as shown by the negative charge of the methylene moiety (−0.16) and the positive charge of the propyl group (+0.21).

Charge distributions of **TS-VIIa** and **TS-VIIb** indicate that the charge transfer from an alkane to the carbene complex takes place to a larger extent in the propane reaction than in the methane reaction, which reflects the relative stability of methyl cation and secondary propyl cation. This is consistent with the more advanced hydride transfer in the propane reaction than that in the methane reaction (length of the forming C^1-H^1 bond is 1.244 Å in **TS-VIIa** and 1.196 Å in **TS-VIIb**).

(b) Orbital Analysis of Rh−Rh−C Bonding. To probe the function of the dinuclear structure of the dirhodium catalyst, we analyzed, in several ways, the nature of the Rh−Rh−C π- and σ-bond systems in **V** (carbene complex) and **TS-VIIa** (methane C−H insertion TS). Important Kohn−Sham orbitals of **V** and localized Kohn−Sham orbital (LO) of **TS-VIIa** are shown in Figure 6. First, LUMO of the complex **V** was found to be exactly what is expected, and composed mainly of the carbene vacant 2p orbital, which accepts rather small back-donation from the Rh^1 $4d_{xz}$ orbital (83.3% in $4d_{xz}$ orbital)[32] to form an extended π^*-system that possesses a strongly electrophilic carbene carbon (Figure 6a). Bond alternation because of interaction of the LUMO with the C−H σ-bonding orbital of methane can be identified in the LO shown in Figure 6b. Thus, the hydride transfer and the C−C bond formation take place as a single event. The approach of the C−H bond to the carbene center is directed by the steric effect of the formate bridge and by the node between the 2p (carbene carbon) and the $4d_{xz}$ (Rh^1 atom) orbitals in the LUMO (see Figure 6a).

There are two ways to describe the Rh−Rh−C σ-system (Ψ_1, Ψ_2, and Ψ_3 in Chart 1). HOMO-19, HOMO-3 (Figure 6c,d), and LUMO+2 (not shown) correspond to Ψ_1, Ψ_2, and Ψ_3, respectively. In one analysis, the Rh^2 nonbonding $4d_{z^2}$ orbital

(32) For NBO analysis of metal-carbene complexes, see: (a) Vyboishchikov, S. F.; Frenking, G. *Chem.-Eur. J.* **1998**, *4*, 1428−1438. (b) Sheehan, S. M.; Padwa, A.; Snyder, J. P. *Tetrahedron Lett.* **1998**, *39*, 949−952.

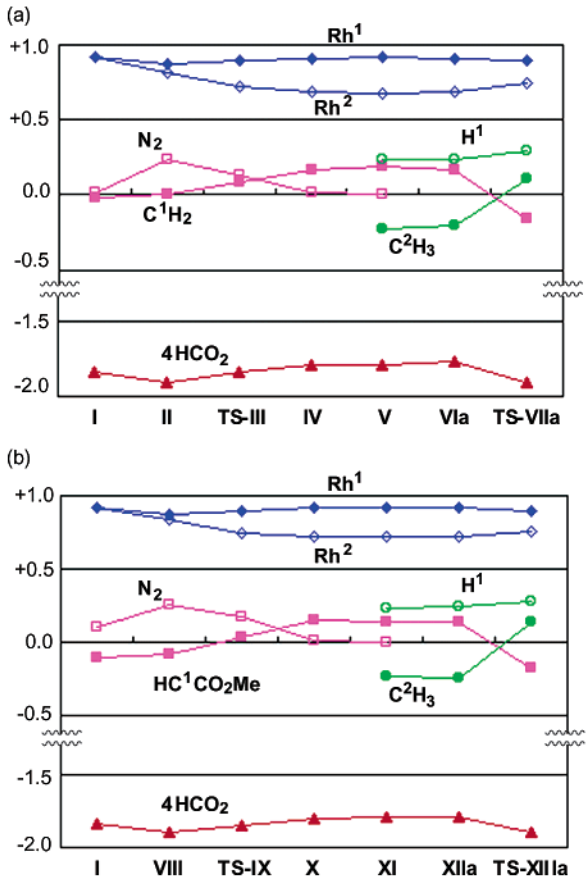

Figure 5. Charge distribution along the reaction coordinate for (a) the reaction between diazomethane and methane and (b) the reaction between methyl diazoacetate and methane.

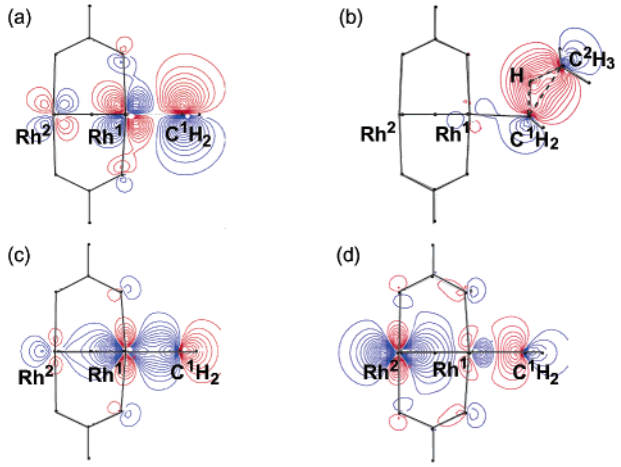

Figure 6. Kohn−Sham orbitals of **V** (a, LUMO; c, HOMO-19; and d, HOMO-3) and LO of **TS-VIIa** responsible for bond alternation (b). The contour intervals are 0.025 e au^{-3}.

interacts with the Rh^1−C^1 σ/σ^*-orbitals (Chart 1a), which weakens the Rh^1−C^1 σ-bond. This interaction is important in the reaction with an alkane, where Rh^2 moves toward Rh^1, and the Rh^1−C^1 bond is being cleaved as the C−H insertion proceeds. In this sense, the Rh^2 atom possessing high-lying 4d$_{z^2}$ electrons is ideally positioned by the carboxylate bridges. In another analysis (Chart 1b), the nonbonding carbene 2sp orbital interacts with the Rh^1−Rh^2 σ/σ^*-orbitals.[33] With this interaction, the Rh^1−Rh^2 bond weakens, and negative charge moves from the carbene to the Rh^2 atom, which accounts for the changes of

Chart 1. Rh−Rh−C σ-System (Ψ_1, Ψ_2, and Ψ_3) Constructed in Two Ways

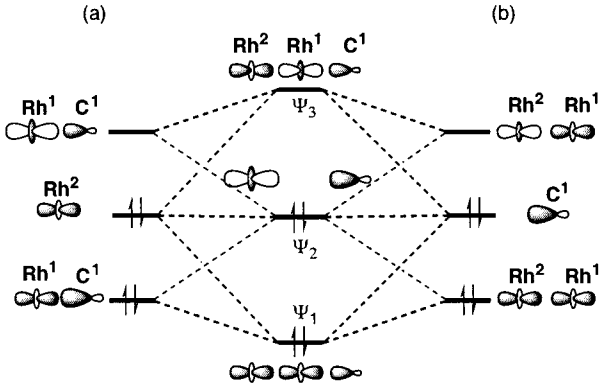

(a) From Rh^2 nonbonding 4d$_{z^2}$ orbital and Rh^1−C^1 σ/σ^*-orbitals, and (b) from Rh^1−Rh^2 σ/σ^*-orbitals and nonbonding carbene 2sp orbital.

Chart 2

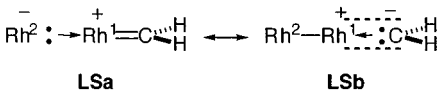

the structure and the charge distribution along the carbene complex formation as discussed above.

The above molecular orbital discussion is supported by the natural bond orbital analysis,[30,32] which indicates that **V** can be described with nearly equal contributions of two resonance structures **LSa** and **LSb** (Chart 2).[34] In the Lewis structure **LSa**, a cationic Rh^1 carbene complex is coordinated with the nonbonding electrons of the Rh^2 atom (indicated as a dative bond arrow). In **LSb**, nonbonding carbene electrons coordinate to the Rh^1−Rh^2 unit, while the vacant carbene 2p orbital forms a π bond with the Rh^1 4d$_{xz}$ orbital ("π-bonding without σ-covalent bond" is expressed as a pair of broken lines).

2. Reaction of Methyl Diazoacetate with Methane and Propane. α-Diazoesters are the most important compounds for the rhodium-catalyzed C−H insertion reaction. In Figure 7 is shown the energy profile of the Rh$_2$(O$_2$CH)$_4$-catalyzed C−H insertion reaction of methyl diazoacetate with methane (denoted as **a**) and propane (CH_3 insertion (denoted as **b**) and CH_2 insertion (denoted as **c**)). The reaction pathway and the energetics obtained for the diazoacetate model are essentially the same as those of the diazomethane model (Scheme 2). The Rh/diazoacetate complex **VIII** forms with 13.0 kcal/mol stabilization energy. The activation energy for the nitrogen extrusion (**TS-IX**) is 16.7 kcal/mol, which is nearly identical with that of the diazomethane model (16.6 kcal/mol). Unlike in the diazomethane model, [**XI** (carbene complex) + N_2] is more stable than **TS-IX** by 3.7 kcal/mol. The C−H activation/C−C formation step proceeds with a moderate (9.8 kcal/mol for methane insertion) or a small (4.7 kcal/mol for propane CH_3 insertion and 0.2 kcal/mol for propane CH_2 insertion) activation energy with large exothermicity (52−54 kcal/mol). The activation energy for propane methylene insertion is much lower than the activation energy for methane insertion, with propane

(33) The energy levels of the Rh^1−Rh^2 σ and σ^* orbital of **I** and the σ-donor orbital of singlet methylene carbene (optimized at the B3LYP/6-31G(d) level) are −9.1, −3.7, and −6.6 eV, respectively, which forms the background of the orbital interaction diagram shown in Figure 6b.

(34) The two Lewis structures **LSa** and **LSb** showed nearly the same percentage of the total electron density (**LSa**, 97.65%; **LSb**, 97.60%), and hence were considered to equally contribute to the nature of the complex.

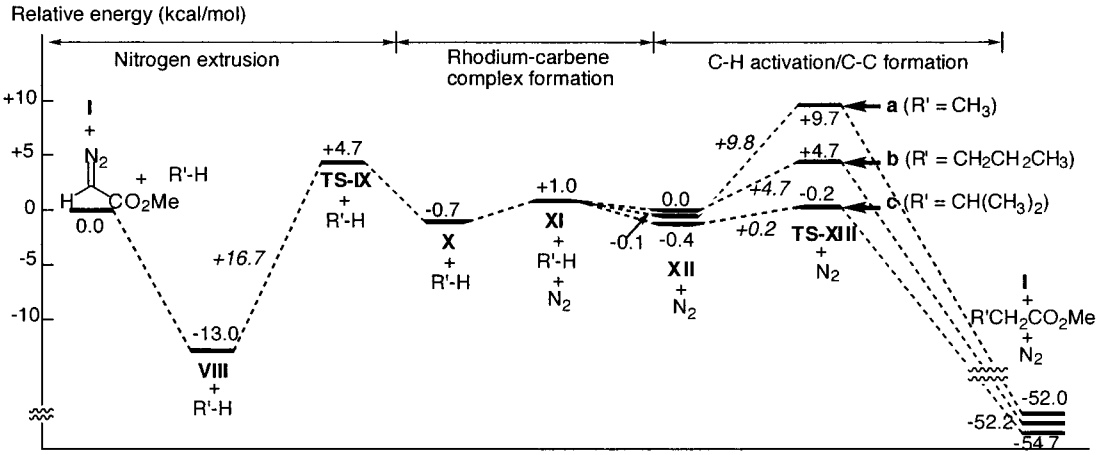

Figure 7. Energy profile of the $Rh_2(O_2CH)_4$-catalyzed reaction of methyl diazoacetate with methane (denoted as **a**) and propane (CH_3 insertion (denoted as **b**) and CH_2 insertion (denoted as **c**)) at the B3LYP/631LAN level.

methyl insertion in between. Details of each reaction step and properties of equilibrium and transition structures will be discussed below.

The 3-D structures of **VIII** and **TS-IX** are shown in Figure 8. The nitrogen extrusion step starts with complex formation between the rhodium catalyst and diazoester (**VIII**).[35,36] HOMO-18 of **VIII** (Figure 8b) illustrates donation from the diazoacetate to the Rh^1-Rh^2 σ^*-orbital. On the other hand, no back-donation from the Rh^1 occupied $4d_{xz}$ orbital to the diazoester was identified in **VIII**. Thus, **VIII** is a simple Lewis acid/Lewis base complex.

In the nitrogen extrusion transition state **TS-IX**, the Rh^1-C^1 bond shortens (2.337 Å → 2.041 Å, 13% decrease), and the C^1-N bond lengthens (1.335 Å → 1.933 Å, 45% increase). In addition, substantial change of hybridization (sp^3 → sp^2) at the C^1 atom takes place from **VIII** to **TS-IX** (sum of bond angles around C^1, 324.0° (**VIII**) → 349.0° (**TS-IXs**)). The charge distribution shows the same tendency as found for the diazomethane model (cf. Figure 5). This is also found in the events after the nitrogen extrusion. As seen in the energy profile of the reaction (Figure 7), **TS-IX** is a very late transition state and shows some character of the rhodium−carbene complex, and back-donative interaction is identified in the LO of **TS-IX** (Figure 8c, **LO2**). This back-donation from the Rh^1 occupied $4d_{xz}$ orbital to the C^1-N σ^*-orbital is an important driving force of the nitrogen extrusion.[5b,9b] The activation enthalpy ($\Delta H^{\ddagger}$) of the nitrogen extrusion (15.2 kcal/mol) is in reasonable agreement with the experimental value (16.4 ± 1.4 kcal/mol, $Rh_2(OAc)_4$ and ethyl diazoacetate).[5a]

The 3-D structure of the dirhodium methoxycarbonyl carbene complex **XI** is shown in Figure 9. The important issue to be addressed here is the influence of the methoxycarbonyl group on the character of the $Rh^2-Rh^1-C^1$ bond system. The carbene carbon center of **XI** is electrophilic, as indicated from the positive charge of the carbene moiety (+0.14) and significant contribution of the 2p orbital of the carbene carbon in the LUMO of **XI** (Figure 9b). One will expect that the carbene carbon of **XI** is more electrophilic than that of the methylene carbene complex (**V**) because **XI** has the electron-withdrawing ester group. On the contrary, the energy levels of LUMO are the same (−3.7 eV) for **V** and **XI**, because the vacant 2p orbital of the carbene carbon of **XI** is *not conjugated* with the ester carbonyl group. There is one notable structural feature in **XI** that is described below.

The Rh^1-C^1 π-bond and the ester carbonyl C^2-O^1 π-bond are orthogonal to each other and not conjugated with each other (the dihedral angle $\angle Rh^1-C^1-C^2-O^1 = 112.0°$).[37,38] This orientation of the ester group has thus far escaped attention of chemists working in this area. For instance, the $Rh^1{=}C^1-C^2{=}O^1$ π-array has often been depicted to be planar and conjugated.[9bc,11b,39] In this structure, the $C^2{=}O^1$ π-bond and the Rh^1-C^1 σ-bond (not the Rh^1-C^1 π-bond) are considered to have some interaction like an α-metaloester. Indeed, one can identify HOMO-22 of **XI** that comprises a four-electron out-of-phase interaction between Rh^1-C^1 σ- and $C^2{=}O^1$ π-orbitals (Figure 9c). Thus, the ester carbonyl group affects the character of the Rh−Rh−C σ-system of the carbene complex rather than that of the π-system. The orthogonal geometry of **XI** described here creates a diastereomerism in the C−H activation stage; a stereochemical issue so far escaped attention (vide infra).

Structural changes around the methane C−H insertion transition state (**TS-XIIIa**) are shown in Figure 10.[40] The potential energy surface is very flat before **TS-XIIIa**, but it is very steep after **TS-XIIIa**. As it goes from [**XI** + methane] to **TS-XIIIa**, positive charge develops in the methane moiety (0.00 → +0.42), and the carbene moiety becomes negatively charged (+0.14 → −0.18). The C−H bond of the methane approaches **XI** to have

(35) Both the *S*-trans and *S*-cis conformers of methyl diazoacetate were examined for the catalyst/diazoacetate complex and the nitrogen extrusion TS from it. The energy differences are very small, and only the result of *S*-trans isomer is shown in this paper.

(36) The existence of such a complex was experimentally demonstrated: Maxwell, J. L.; Brown, K. C.; Bartley, D. W.; Kodadek, T. *Science* **1992**, *256*, 1544−1547.

(37) Similar structures were found in ruthenium alkoxycarbonyl carbene complexes: Nishiyama, H.; Aoki, K.; Itoh, H.; Iwamura, T.; Sakata, N.; Kurihara, O.; Motoyama, Y. *Chem. Lett.* **1996**, 1071−1072. Galardon, E.; Le Maux, P.; Toupet, L.; Simonneaux, G. *Organometallics* **1998**, *17*, 565−569.

(38) Such orientation of ester carbonyl group was also noted in theoretical studies of copper-catalyzed cyclopropanation reaction with α-diazoester: Fraile, J. M.; García, J. I.; Martínez-Merino, V.; Mayoral, J. A.; Salvatella, L. *J. Am. Chem. Soc.* **2001**, *123*, 7616−7625.

(39) Examples: Timmons, D. J.; Doyle, M. P. *J. Organomet. Chem.* **2001**, *617*−*618*, 98−104. Bulugahapitiya, P.; Landais, Y.; Parra-Rapado, L.; Planchenault, D.; Weber, V. *J. Org. Chem.* **1997**, *62*, 1630−1641.

(40) For the methane reaction, two diastereomeric TSs were located. Only one of the two is shown in this paper because the energy difference was very small (0.2 kcal/mol).

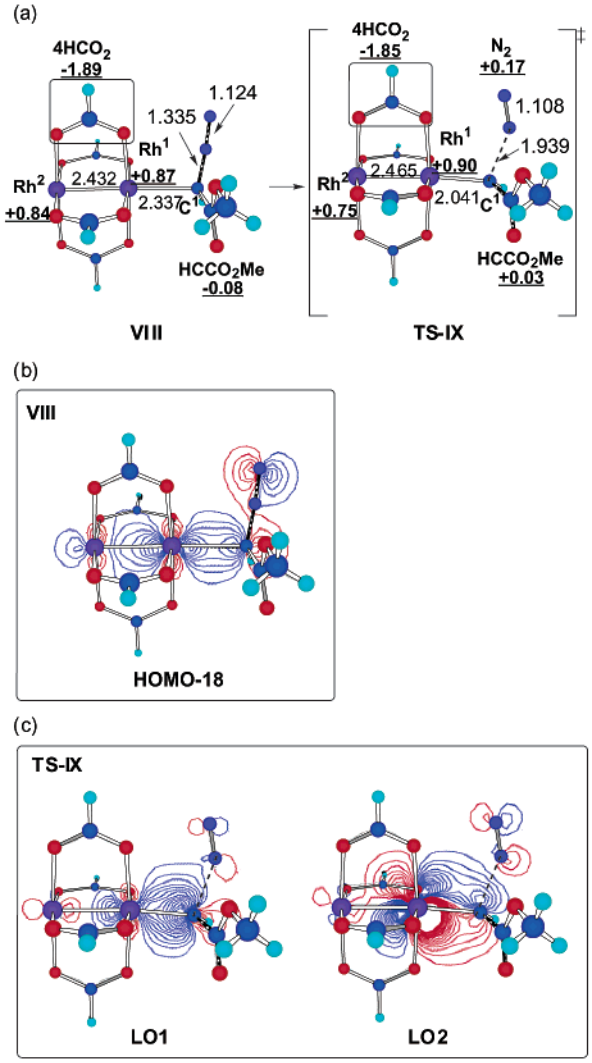

Figure 8. (a) 3-D structures of the $Rh_2(O_2HC)_4$/methyl diazoacetate complex **VIII** and the nitrogen extrusion TS (**TS-IX**) optimized at the B3LYP/631LAN level. The numbers refer to bond lengths (Å) and natural charges (underlined). (b) HOMO-18 orbital of **VIII** indicating donative interaction. (c) Localized orbitals of **TS-IX** indicating donative (**LO1**) and back-donative (**LO2**) interaction. Orbitals are shown in the Rh^1-C^1-N plane, and contour intervals are 0.025 e au^{-3} for HOMO-18 and **LO1**, 0.010 e au^{-3} for **LO2**.

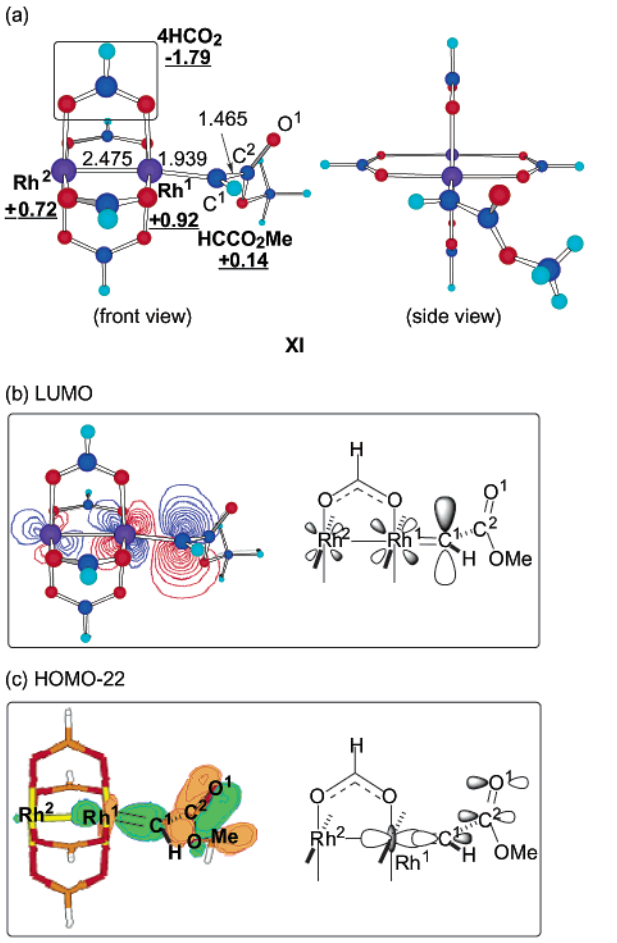

Figure 9. (a) 3-D structure of the dirhodium methoxycarbonyl carbene complex **XI** optimized at the B3LYP/631LAN level. The numbers refer to bond lengths (Å) and natural charges (underlined). (b) The contour map of LUMO and (c) the surface of HOMO-22 of **XI** and their schematic representations. The orbitals are shown in the $Rh^1-Rh^2-C^1$ plane. The contour interval for (b) is 0.025 e au^{-3}, and the contour value for (c) is 0.060 e au^{-3}.

maximum interaction with the LUMO (Figure 9b), and the LO of **TS-XIIIa** shows three-centered interaction between the C^3-H^1 σ-orbital of methane and the vacant 2p orbital of the carbene carbon C^1. The C−H activation is an electrophilic reaction, and the bond alternation including the $C^1-H^1-C^3$ moiety takes place as a single event in **TS-XIIIa**. Despite a previous suggestion that the Rh^1 atom may interact with the C−H bond,[11b] we could not locate such a TS. Such a TS is difficult to achieve because of electronic and steric reasons; that is, there is a node in the LUMO of **XI** (Figure 9b), and the Rh^1 atom is sterically too congested to interact with any nucleophile.

Changes of the lengths of breaking C−H bond, forming C−H bond, and forming C−C bond along the IRC (Figure 10) indicate nonsynchronicity of the C−H bond activation/C−C bond formation stage. In the structure of $s = +1.7$ $amu^{1/2}$ bohr from **TS-XIIIa**, the C^1-H^1 bond is completely formed (1.10 Å), but the C^1-C^2 bond is yet to be formed (1.92 Å). The Rh^1-C^1 bond becomes much elongated near **TS-XIIIa** (2.028 → 2.126 → 2.277 Å), while the change of the Rh^1-Rh^2 bond length is small.

The activation energy of the C−H insertion is rather high with methane (9.8 kcal/mol), moderate (4.7 kcal/mol) with propane (CH_3 insertion), and extremely low (0.2 kcal/mol) with propane (CH_2 insertion). This parallels the experimental fact that the reactivity of a C−H bond increases in an order of primary, secondary, and tertiary.[7] Three TSs of C−H activation shown in Figure 11 are compared. The net positive charges of alkyl groups are +0.14, +0.20, and +0.25 in **TS-XIIIa** (methane insertion), **TS-XIIIb** (propane CH_3 insertion), and **TS-XIIIc** (propane CH_2 insertion), respectively. These values are consistent with the stability order of the incipient carbocation (methyl < primary < secondary).

Bond lengths also give important information on the C−H activation/C−C formation reaction. Lengths of the breaking C−H bonds are 1.234, 1.281, and 1.324 Å, and those of forming C−H bonds are 1.275, 1.232, and 1.210 Å for **TS-XIIIa**, **TS-XIIIb**, and **TS-XIIIc**, respectively. Thus, hydrogen transfer is the most advanced in the propane CH_2 insertion. On the other hand, the C−C bond formation is the most advanced in the methane reaction (C−C distance: 2.200, 2.208, and 2.282 Å for **TS-XIIIa**, **TS-XIIIb**, and **TS-XIIIc**, respectively). Putting

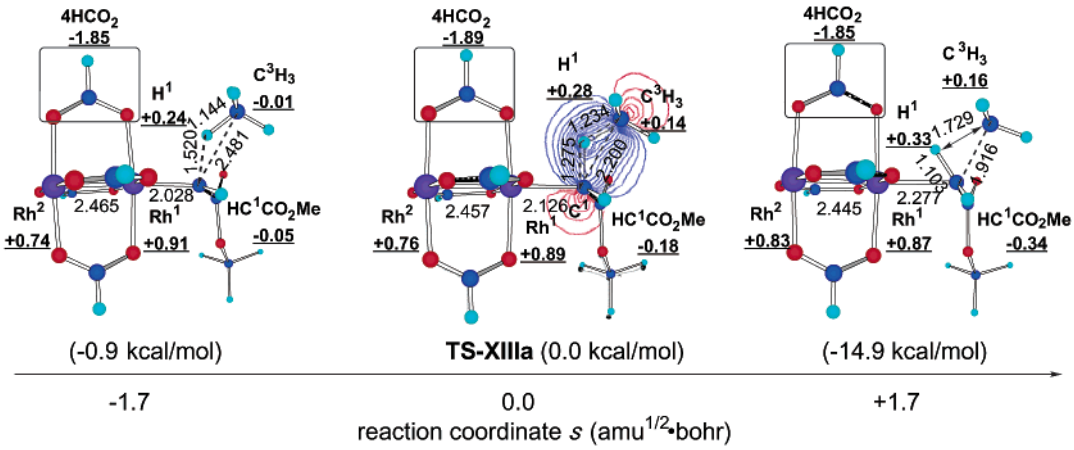

Figure 10. 3-D structures of methane C−H insertion TS (**TS-XIIIa**) and intermediary structures on the IRC of both forward (+1.7 amu$^{1/2}$ bohr) and reverse (−1.7 amu$^{1/2}$ bohr) direction at the B3LYP/631LAN level. The numbers refer to bond lengths (Å) and natural charges (underlined). The localized orbital of **TS-XIIIa** is shown together with its 3-D structure.

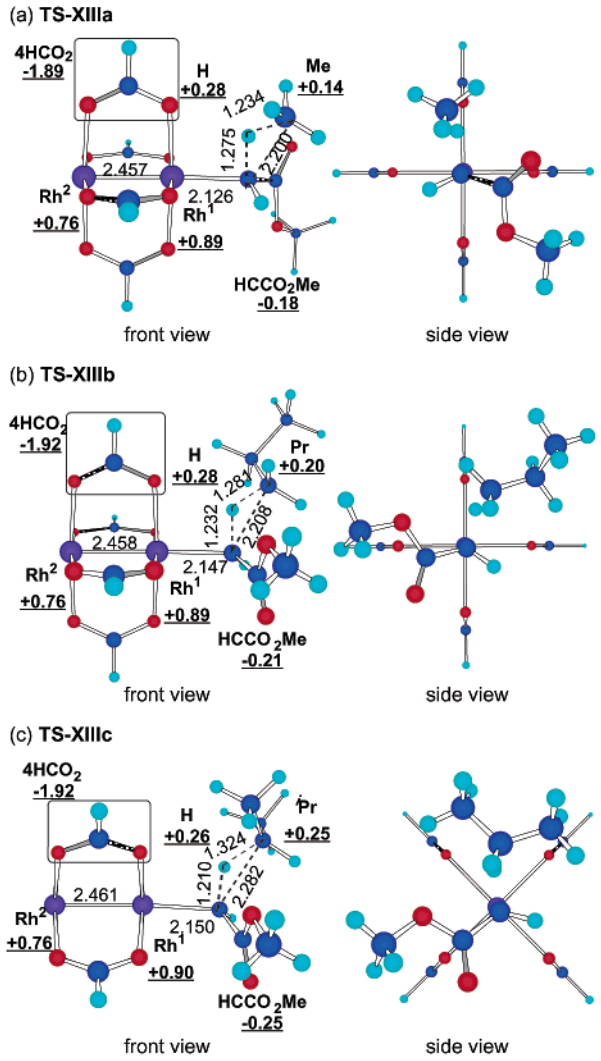

Figure 11. 3-D structures of the C−H insertion TSs of (a) methane (**TS-XIIIa**), (b) propane (CH_3, **TS-XIIIb**), and (c) propane (CH_2, **TS-XIIIc**) with the carbene complex **XI** optimized at the B3LYP/631LAN level. The numbers refer to bond lengths (Å) and natural charges (underlined).

all these data together, one can conclude that the C−H activation/C−C bond formation process is a nonsynchronous concerted reaction bearing a character of hydride abstraction. It should be pointed out that the Rh^1−C^1 bond of the carbene complex **XI** (1.939 Å) is much elongated in the C−H insertion TSs (2.126−2.150 Å, about 10% increase).

Kinetic isotope effects (KIEs) data have proven to be useful to correlate the nature of the TSs inferred by experiments and by theory.[41] The KIE calculated for the insertion to secondary C−H/C−D bond of propane/propane-d_8 was found to be 2.03 (eq 3), which can be favorably compared with the experimental data. The KIE values of 2.45 and 1.55 were reported for the reaction of ethyl diazoacetate with a cyclohexane/cyclohexane-d_{12} pair under the catalysis of $Rh_2(OAc)_4$ and $Rh_2(OCOCF_3)_4$, respectively.[6a] The correlation looks reasonable because the electron-withdrawing ability of the formate ligand falls between that of acetate and trifluoroacetate ligands (i.e., inversely related to the acidity of the conjugate acid).[42]

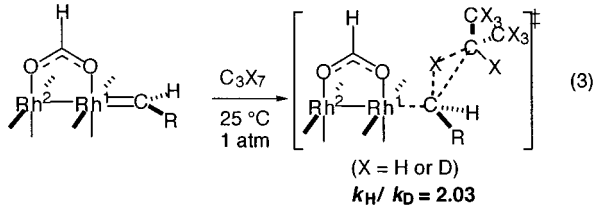

(3)

3. Enthalpy and Gibbs Free Energy Profiles of the Catalytic Cycles. The enthalpies and the Gibbs free energies of the present reactions were calculated for the structures optimized at the B3LYP/631LAN level. The enthalpy (a) and the Gibbs free energy profiles (b) of the diazomethane model are shown in Figure 12. When free energies are considered (Figure 12b), the complex between **V** (carbene complex) and N_2 (**IV**) becomes no longer more stable than [**V** + N_2]. The complexes between **V** and an alkane (methane (**VIa**) or propane (**VIb**)) also become less stable than [**V** + R′−H]. Therefore, these complexes may not exist as stable intermediates in actual reactions (therefore omitted from Figure 12).[43] While the thermal correction for enthalpy did not change

(41) Examples: DelMonte, A. J.; Haller, J.; Houk, K. N.; Sharpless, K. B.; Singleton, D. A.; Strassner, T.; Thomas, A. A. *J. Am. Chem. Soc.* **1997**, *119*, 9907−9908. Frantz, D. E.; Singleton, D. A. *J. Am. Chem. Soc.* **2000**, *122*, 3288−3295.
(42) Bordwell, F. G. *Acc. Chem. Res.* **1988**, *21*, 456−463.
(43) Rapid and reversible complexation between a rhodium-carbene complex and a C−H bond is assumed in ref 11a.

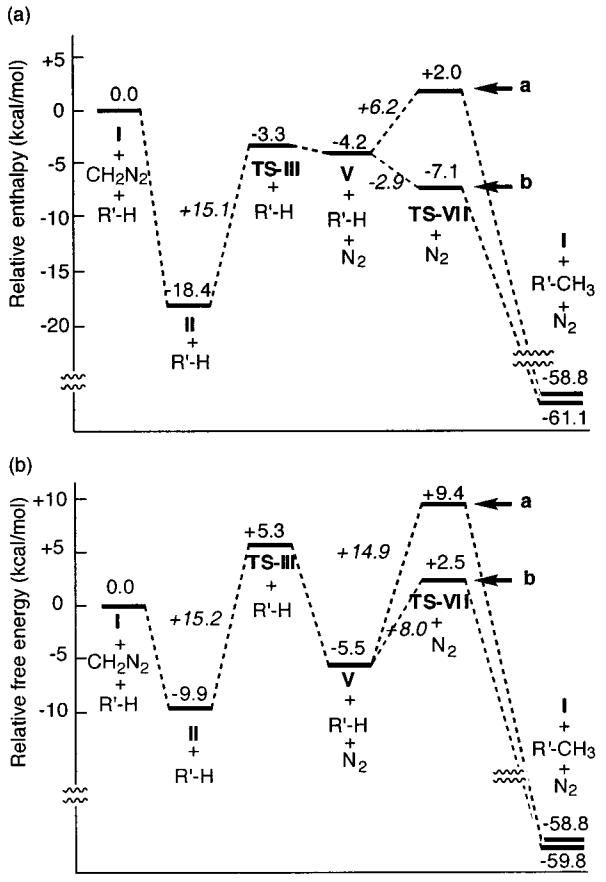

Figure 12. (a) Enthalpy and (b) Gibbs free energy profiles of the $Rh(O_2CH)_4$-catalyzed reaction of diazomethane with methane and propane, obtained with the structures optimized at the B3LYP/631LAN level.

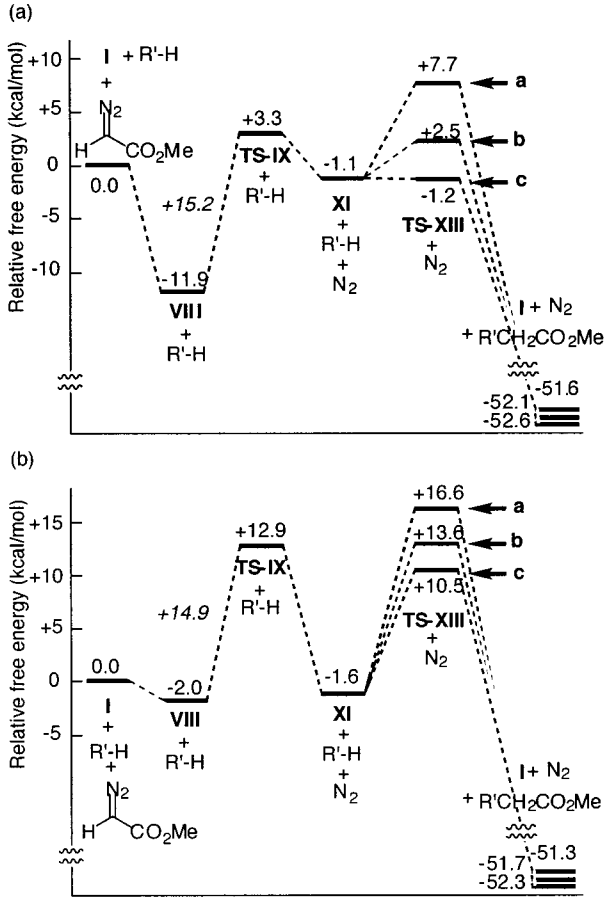

Figure 13. (a) Enthalpy and (b) Gibbs free energy profiles of $Rh_2(O_2CH)_4$-catalyzed reaction of methyl diazoacetate with methane and propane, obtained with the structures optimized at the B3LYP/631LAN level.

the energy profile very much (Figures 3 and 12a), consideration of the entropy term expectedly changes the energy profile (Figure 12b). The stabilization energy of the complexation between **I** and diazomethane has become 9.9 kcal/mol, whereas the activation energy of the nitrogen extrusion (15.2 kcal/mol) is not much affected. The carbene complex [**V** + N_2] becomes much more stable than the nitrogen extrusion TS (**TS-III**). The activation energies of the C−H insertion (the energy difference between [**V** + R′−H] and **TS-VII**) significantly increase.

The enthalpy (a) and the Gibbs free energy profiles (b) of the diazoester model are shown in Figure 13. Similar to the diazomethane model, the entropy term exerts a considerable influence on the free energy changes, especially on the activation energy of the C−H insertion step. The activation energy of the nitrogen extrusion step was not affected very much again. In accordance with experiments, the nitrogen extrusion step was found to be the rate-limiting for the secondary C−H insertion reaction (Figure 13b).[44]

Discussion

The present studies have revealed, for the first time, the energetics, the electronic nature, and the 3-D structures of the intermediates and the TSs in the catalytic cycle of the dirhodium tetracarboxylate-catalyzed C−H bond activation/C−C bond formation reaction (Scheme 3). Some pertinent experimental data have been reasonably reproduced by the DFT calculations, that is, the activation enthalpy of the rate-limiting nitrogen extrusion, relative reactivity of C−H bonds, and the kinetic isotope effect of the C−H insertion step. The nature of the C−H activation/C−C formation step, which has so far been little known, was found to be concerted but nonsynchronous. Two important events are taking place in the concerted, nonsynchronous TS as illustrated with two resonance structures (bracket in Scheme 3). The first event is the hydride transfer from the alkane to the carbene carbon. The second is the C−C bond formation and the regeneration of the Rh−Rh bond. The Rh atoms do not directly interact with the alkane C−H bond. Thus, the mechanism of the carbene complex reaction is different from those of other C−H activation reactions that involve metal/C−H bond interaction.[45,46]

The molecular orbital and NBO analyses combined with the known experimental data[5−9] indicate that the C−H insertion comprises an electrophilic attack of the carbene 2p orbital onto the C−H σ-bonding orbital of an alkane. The reaction proceeds through a relatively late TS, where the Rh^1-C^1 bond cleavage is therefore involved. This appears to be general for the C−H bond activation reaction of metal carbene complexes (vide infra)

(44) For the methane insertion, the C−H activation step was calculated to be rate-limiting as shown in Figure 13b. Experimental investigation of methane insertion has not been reported, and it may be true that the C−H activation is the rate-limiting step in this reaction.

(45) Weiller, B. H.; Wasserman, E. P.; Bergman, R. G.; Moore, C. B.; Pimentel, G. C. *J. Am. Chem. Soc.* **1989**, *111*, 8288−8290. Wasserman, E. P.; Moore, C. B.; Bergman, R. G. *Science* **1992**, *255*, 315−318.

(46) Koga, N.; Morokuma, K. *J. Phys. Chem.* **1990**, *94*, 5454−5462.

Scheme 3

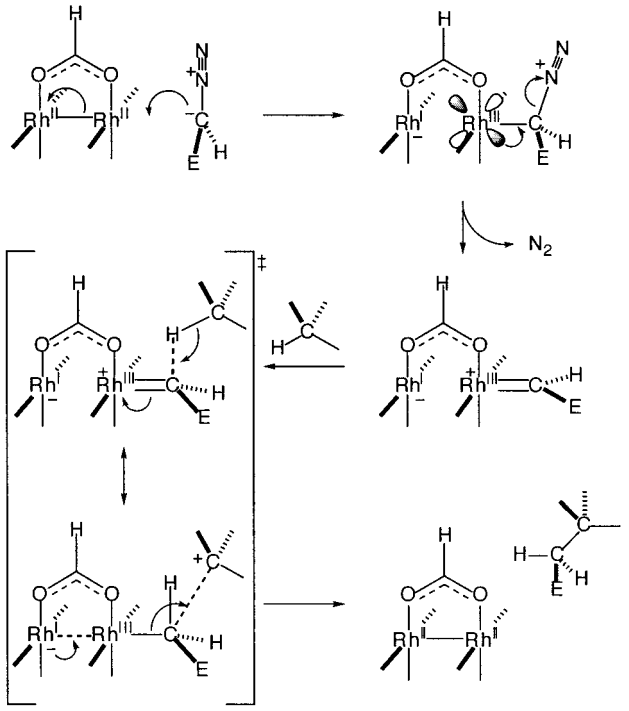

and metal carbenoids and represents the difference between the C−H insertion reaction and their cyclopropanation reaction. The TS of the latter reaction involves a much earlier transition state (i.e., little metal−carbene bond cleavage was found by us and by Salvatella et al.).[38,47] For the reaction with such a nucleophilic substrate as an olefin, the electrophilicity of the carbene carbon atom controls the reaction. On the other hand, in the C−H activation, the lability of the metal−carbene σ-bond in the TS is as important as the high electrophilicity of the carbene carbon.

We consider that the structure of the dirhodium complex **I** is ideal for the C−H bond activation reaction, because the Rh^2 atom acts as a bifunctional electron pool (Scheme 3). Thus, the Rh^2 atom is detached from the Rh^1-C^1 moiety to enhance the electrophilicity of the carbene center (net result is charge transfer from the carbene to the Rh^2 atom and formation of a formal cationic Rh^1−carbene complex as shown in Chart 2) or attached to it to facilitate the cleavage of the Rh^1-C^1 bond in the transition state (loosening of the Rh^1-C^1 bond). The carboxylate groups serve as anchors of the Rh^2 atom and also as electron-withdrawing groups that enhance the electrophilicity of the carbene center. It also serves as the site to harness chirality. Much related synergistic effects of two equal transition metals have also been pointed out for the $Co_2(CO)_8$-catalyzed Pauson−Khand reaction.[48]

To further probe the role of the dinuclear structure, the rhodium reaction was compared with single metal model reactions. Methane C−H insertion reactions of copper−[49] (**XIV**) and ruthenium−methylene carbene complexes (**XVI**)[50] were briefly studied (eqs 4 and 5).[51,52] The activation energy of the C−H insertion is 15.6 kcal/mol for **XIV**, and 27.6 kcal/mol for **XVI**, values much higher than that for the dirhodium carbene complex **V** (+5.7 kcal/mol).[53]

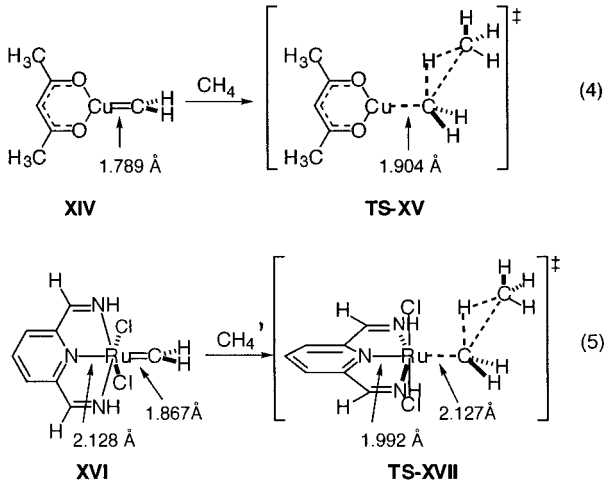

Significant metal−carbon bond cleavage is found in the C−H insertion TSs (**TS-XV** and **TS-XVII**) as found for the rhodium−carbene complex (eqs 4 and 5, see also Figure 3). The N (pyridine)−Ru bond shortens by 6.4% (2.128 → 1.992 Å) as the carbene group is transferred to methane.

One may consider that the trans effect of the ligand in these complexes might play significant roles in the C−H insertion reaction. In the Cu complex **XIV**, there is no ligand trans to the carbene group. In the Ru complex **XVI**, a pyridine ligand is positioned trans to the carbene ligand and facilitates the Ru−C bond cleavage. However, its effect must be rather weak because the lone pair of the nitrogen atom is a weak donor to the Ru−C σ*-orbital. The Rh^2 atom in **V** causes a much stronger trans effect to the neighboring Rh^1-C^1 σ*-orbital, because the Rh^2 nonbonding $4d_{z^2}$ orbital is energetically very close to the Rh^1-C^1 σ*-orbital (cf. Chart 1).

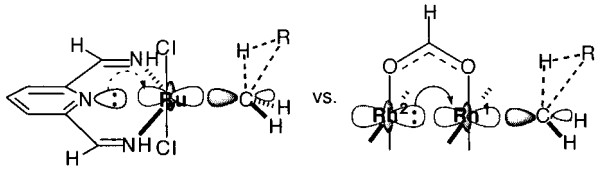

A minor but intriguing feature of the rhodium−carbene complexes **V** and **XI** is the facile rotation around the Rh^1-C^1 axis. The energy gaps between an eclipsed conformer (minimum) and a staggered one (transition state of the rotation) are only 1.1 kcal/mol (diazomethane model) and 0.7 kcal/mol (diazoester model). The dirhodium tetracarboxylate moiety being D_4 symmetric, the Rh^1 $4d_{xz}$ and $4d_{yz}$ orbitals are degenerate. Thus, either $4d_{xz}$ or $4d_{yz}$, or their hybrid orbitals, can contribute to the back-donation to the carbene vacant 2p orbital, and

(47) Nakamura, E.; Hirai, A.; Nakamura, M. *J. Am. Chem. Soc.* **1998**, *120*, 5844−5845.
(48) Yamanaka, M.; Nakamura, E. *J. Am. Chem. Soc.* **2001**, *123*, 1703−1708.
(49) Nozaki, H.; Moriuti, S.; Yamabe, M.; Noyori, R. *Tetrahedron Lett.* **1966**, 59−63. Wulfman, D. S.; McDaniel, R. S.; Peace, B. W. *Tetrahedron* **1976**, *32*, 1241−1249.
(50) Nishiyama, H.; Itoh, Y.; Matsumoto, H.; Park, S.-B.; Itoh, K. *J. Am. Chem. Soc.* **1994**, *116*, 2223−2224.
(51) The B3LYP method was employed for geometry optimization. The basis sets used are as follows: the Ahlrichs SVP set (ref 52) for Cu, the LANL2DZ set for Ru, and the 6-31G(d) sets for the rest.
(52) Schäfer, A.; Horn, H.; Ahlrichs, R. *J. Chem. Phys.* **1992**, *97*, 2571−2577.
(53) Recently an efficient Cu(I)-catalyzed C−H insertion reaction has been reported: Díaz-Requejo, M. M.; Belderraín, T. R.; Nicasio, M. C.; Trofimenko, S.; Pérez, P. J. *J. Am. Chem. Soc.* **2002**, *124*, 896−897.

Chart 3

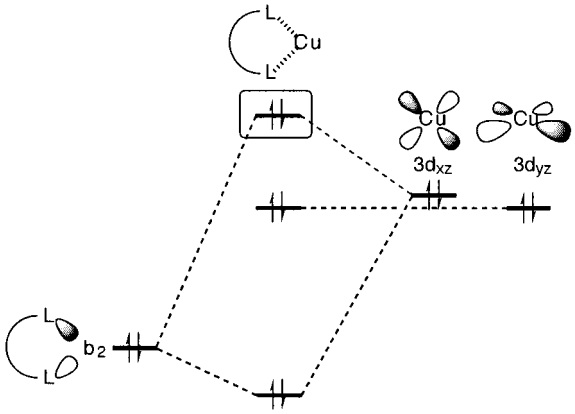

therefore the back-donation scheme can operate for any Rh^1-C^1 bond rotational isomers.

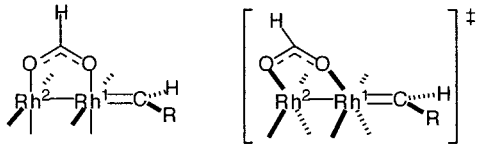

Copper(I)−bidentate ligand complex is different. The bent structure of the acetylacetonato ligand on the Cu(I) atom pushes up the Cu $3d_{xz}$ orbital (Chart 3).[54] Hence, only the $3d_{xz}$ orbital can effectively contribute to the back-donation to the carbene. The rotation around the Cu−C bond therefore becomes difficult in the copper−carbene complex. The activation energy of the carbene ligand rotation of **XIV** is calculated to be 13.5 kcal/mol.

The final issue of note is the geometry of the ester group in the carbene complex **XI**; that is, the carbonyl C^2-O^1 π-bond and the Rh^1-C^1 π-bond are orthogonal to each other and therefore not conjugated with each other. When the carbene complex was optimized with C_s symmetry restriction (keeping the $Rh^1{=}C^1-C^2{=}O^1$ moiety in a plane; this structure is denoted as **XI-*C*$_s$**), **XI-*C*$_s$** was less stable than **XI** by 6.4 kcal/mol. The C^1-C^2 bond length of **XI** (1.465 Å) is shorter than that of **XI-*C*$_s$** (1.495 Å). Putting together this result and the orbital interaction shown in Figure 9c, we conclude that the C^2-O^1 π-bond is conjugated with the Rh^1-C^1 σ-bond (instead of the Rh^1-C^1 π-bond).

(54) Mori, S.; Nakamura, E. *Tetrahedron Lett.* **1999**, *40*, 5319−5322. Mori, S.; Hirai, A.; Nakamura, M.; Nakamura, E. *Tetrahedron* **2000**, *56*, 2805−2809.

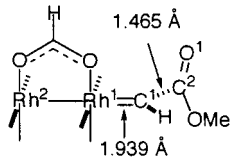

XI

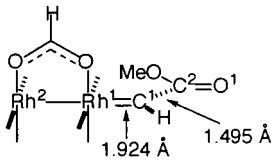

XI-*C*$_s$

As a result, the two faces of the carbene moiety become no longer equivalent to each other. Therefore, there exist two approaches of a C−H bond to the carbene moiety. The difference of the two pathways will become significant when a bulky substituent is used for the ester group. Previous interpretations of stereoselectivity of both intra- and intermolecular C−H insertion reactions may need reconsideration because they often neglect this geometrical feature of the carbene complex.

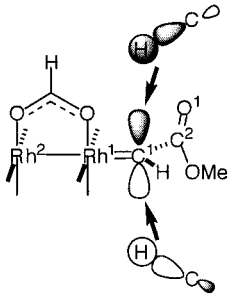

In summary, the present study revealed the mechanisms of the C−H insertion reaction of a diazo compound with an alkane catalyzed by a dirhodium tetracarboxylate complex. The theoretical analysis delineated above will contribute to the rational designing of useful synthetic transformations. Further theoretical studies of stereoselective inter- and intramolecular C−H insertion reactions are in progress.[55]

Acknowledgment. We thank the Ministry of Education, Culture, Sports, Science, and Technology for financial support (Grant-in-Aid for Scientific Reserch, Specially Promoted Research). Generous allotment of computational time from the Institute for Molecular Science, Okazaki, Japan, and the Intelligent Modeling Laboratory, the University of Tokyo, is gratefully acknowledged.

Supporting Information Available: Cartesian coordinates of the representative stationary points (PDF). This material is available free of charge via the Internet at http://pubs.acs.org.

JA017823O

(55) For 3-D structures and coordinates, see: http://www.chem.s.u-tokyo.ac.jp/~common/Theo/Rh2/title.